ELSEVIER

Thermochimica Acta 371 (2001) 95–101

thermochimica acta

www.elsevier.com/locate/tca

Use of SnO for the determination of standard Gibbs energy of formation of SnO_2 by oxide electrolyte e.m.f. measurements

C. Mallika[a], A.M. Edwin Suresh Raj[b], K.S. Nagaraja[b], O.M. Sreedharan[a,*]

[a]*Thermodynamics and Kinetics Division, Indira Gandhi Centre for Atomic Research, Kalpakkam, Tamil Nadu 603 102, India*
[b]*Department of Chemistry, Loyola Institute of Frontier Energy, Loyola College, Chennai, Tamil Nadu 600 034, India*

Received 7 September 2000; accepted 12 December 2000

Abstract

Evidence was obtained from DTA for the disproportionation of SnO into Sn(l) and SnO_2 at 815 K below a heating rate of 20°C/min in helium and at 800 K in air at 10°C/min heating rate. The e.m.f. of a galvanic cell with SnO/SnO_2 and $Sn(l)/SnO_2$ as electrodes using 15 mol% $YO_{1.5}$ stabilised ZrO_2 (15 YSZ) as the electrolyte showed SnO disproportionation into Sn and SnO_2 to be complete by about 750 K. The e.m.f. of the galvanic cells with SnO/SnO_2 as the test electrode, N_2 ($P_{O_2} \approx 10^{-3}$ atm)/Pt or Fe/Fe_xO as the reference electrodes and with 15 YSZ as the electrolyte measured over the ranges 776–1140 and 772–1206 K, respectively, yielded the expression $\Delta G_f^0(SnO_2) \pm 2.2\,(\mathrm{kJ\,mol^{-1}}) = -568.9 + 0.2007T\,(\mathrm{K})$ for the standard Gibbs energy of formation of SnO_2. A third-law analysis of the e.m.f. data yielded $-578.3 \pm 4.0\,\mathrm{kJ\,mol^{-1}}$ for the standard enthalpy of formation, $\Delta H_{f,298}^0$ of $SnO_2(s)$. © 2001 Elsevier Science B.V. All rights reserved.

Keywords: SnO disproportionation; Oxide e.m.f. on SnO; SnO_2 Gibbs energy

1. Introduction

Impedance studies have been reported in the literature on thin films of β-Sn with SnO and SnO_2 for humidity sensing applications [1]. Recently, Edwin Suresh Raj et al. [2] have reported the humidity sensing properties of SnO_2–$SnMoO_4$ composites. Extensive thermoanalytical studies on Sn and its oxides had also been reported [3–8] and although several solid electrolyte e.m.f. measurements have so far been reported [9–18] for the evaluation of the standard Gibbs energy of formation, ΔG_f^0 of SnO_2 at higher temperatures, there is still considerable scatter in the Gibbs energy data and indications of temperature dependent errors in the derived standard enthalpy of formation, $\Delta H_{f,298}^0$ of SnO_2. In an attempt to resolve these discrepancies, this investigation was undertaken. Further, in all the e.m.f. measurements reported in the literature, a mixture of Sn(l) and SnO_2 constituted the test electrode and in no study, pure SnO was used as the starting material. Therefore, in the present investigation, SnO/SnO_2 was used as the test electrode to assess the temperature of complete dissociation into Sn and SnO_2 appropriately corroborated by thermoanalytical studies.

2. Experimental procedure

The starting materials were spectrographically pure Sn granules (DSC standard material, Perkin-Elmer, Switzerland), iron sponge (purity better than 99.9%, Cerac, USA), Fe_2O_3 (purity >99.99%, Johnson

---

[*] Corresponding author. Fax: +91-4114-40301.
E-mail address: oms@igcar.ernet.in (O.M. Sreedharan).

PII: S0040-6031(01)00416-6

Matthey, UK) and SnO (total metallic impurities <0.1%, Fluka, Switzerland). Tin(IV) oxide was made by oxidising SnO in air at 1000 K for 24 h. Powders of SnO and SnO_2 in the mole ratio of 9:1 were mixed and compacted into cylindrical pellets of 10 mm diameter and 2–3 mm thickness at a pressure of 100 MPa. Likewise, electrode pellets of Sn/SnO_2 were made of Sn(s) and SnO_2 in the mass ratio of 4:1. The preparation of Fe/Fe_xO electrode pellets was described elsewhere [19]. A cylindrical solid electrolyte tube with one end closed and closed end flat conforming to the dimensions of outer diameter 12.7 mm, inner diameter 9.8 mm and length 350 mm as well as a solid electrolyte cup with the dimensions of outer diameter 10 mm, inner diameter 7 mm and depth 5 mm with a flat bottom were made of 15 mass% $YO_{1.5}$ stabilised ZrO_2 (15 YSZ, Nippon Kagaku Togyo, Japan). The tube electrolyte was used in the galvanic cells (II) and (III) and the cup electrolytes in the cells (I) and (IV).

A horizontal TG/DTA system, Model-Seiko 320 was used for non-isothermal oxidation studies on SnO up to 1273 K in air at a heating rate of 10°C/min. The TG/DTA of SnO in dynamic helium (P_{O_2} of the order of 1 Pa) was recorded at 20°C/min heating/cooling rate over 2–3 cycles.

The e.m.f. of the galvanic cells

$$\mathrm{Pt, C, SnO, SnO_2|15\,YSZ|SnO_2, Sn(l), C, Pt} \quad \text{(I)}$$

$$\mathrm{Pt, C, SnO, SnO_2|15\,YSZ|N_2}\ (P_{O_2} \approx 10^{-3}\ \mathrm{atm}), \mathrm{Pt} \quad \text{(II)}$$

$$\mathrm{Pt, N_2}\ (P_{O_2} \approx 10^{-3}\ \mathrm{atm})|\mathrm{15\,YSZ|air}\ (P_{O_2} = 0.21\ \mathrm{atm}), \mathrm{Pt\ and} \quad \text{(III)}$$

$$\mathrm{Pt, Fe, Fe_xO|15\,YSZ|SnO, SnO_2, C, Pt} \quad \text{(IV)}$$

were studied over the ranges 753–1000, 776–1140, 788–965 and 772–1206 K, respectively. Purified He was used as the cover gas. The temperature was measured using a Pt–10 mass% Rh/Pt thermocouple calibrated at the freezing temperatures of high-purity metals such as Sn, Zn, Sb and Ag. Other details of the experiments including voltage measurement, tests for the absence of asymmetric potentials, details for purification of helium and temperature control are the same as reported elsewhere [20,21].

3. Results and discussion

3.1. TG/DTA studies

The TG studies were mainly conducted for a preliminary estimation of the temperature range for the existence of SnO in air and in a relatively inert atmosphere in order to fix the operating parameters for the galvanic cell studies. The results of these TG/DTA studies on SnO are summarised in Table 1. It was seen from non-isothermal oxidation studies at a heating rate of 10°C/min that the oxidation of SnO commenced at 612 K and 98% of the total weight gain up to 1263 K was complete by 1030 K. The final product was found to be SnO_2 with a speck of Sn. Since the weight gain from 612 K was more or less gradual up to 1030 K without any significant stepwise change in weight at a given temperature, one would not expect an exotherm corresponding to oxidation. However, there was a sharp exotherm at 800 K which should therefore be attributable to the disproportionation of SnO into Sn and SnO_2. The shape of the TG curve did not warrant any inference such as the formation of an intermediate phase, Sn_3O_4 although no attempt was made to quench

Table 1
TG/DTA study of SnO

S. No.	Conditions	TG	DTA	Inference
1	Static air			
	Heating rate: 10°C/min	612–1030 K, weight gain	Exotherm at 800 K	Disproportionation; SnO_2 with Sn traces
	Heating rate: 10°C/min	1030–1263 K, less than 2% of total weight gain	–	Partial oxidation of Sn
2	Helium ($P_{O_2} \leq 1$ Pa), heating rate: 20°C/min			
2a	First heating	540–815 K, weight gain: 2–3%	Exotherm at 815 K	$2SnO \rightarrow Sn + SnO_2$
2b	First cooling	930–453 K, weight gain: 1%	Exotherm at 489 K	Freezing of Sn
2c	Second heating	334–800 K, weight gain: 0.5%	Endotherm at 500 K	Melting of Sn

a sample from about 810 K for phase identification. Survey of literature revealed that several techniques were employed in investigating the disproportionation of SnO including Mössbauer [22] and TEM [3] besides conventional XRD [5,8,12] and DSC [6]. In some of these studies, an environment depleted with respect to oxygen to the extent of about 10^{-8} atm (1 mPa) of P_{O_2} was used to prevent the oxidation of Sn.

In the second part of the investigation, high purity helium gas with a P_{O_2} of 10^{-5} atm (1 Pa) was only used which would not prevent simultaneous partial oxidation of SnO. However, some of the investigations on SnO mentioned earlier pointed out the formation of an intermediate oxide, Sn_3O_4 prior to final oxidation to SnO_2. In contrast, a study on the aerial oxidation of thin films of Sn at 483 K by Dolotov et al. [8] for more than 20 h revealed the formation of amorphous SnO_2 which crystallised on further heating to 723 K as observed by XRD. This observation showed that given sufficient time and surface area, Sn could be aerially oxidised to SnO_2 at lower temperatures without forming Sn_3O_4.

To identify the disproportionation temperature of SnO by suppressing extensive oxidation (which is a side reaction), a TG/DTA run was taken on a sample of 90 mg of SnO at a heating rate of 20°C/min in dynamic helium ($P_{O_2} \approx 1\,\text{Pa}$) at a flow rate of $10\,\text{dm}^3$/h. This run showed the temperature of disproportionation to be 815 K and the formation of Sn was confirmed by a freezing exotherm at 489 K of super cooled tin in the first cooling cycle, which was further confirmed by the melting endotherm at 500 K in the second heating cycle (Table 1), in addition to verification by XRD up on completion of the DTA run.

From the foregoing discussions it is inferred that if SnO was to be used to determine the equilibrium P_{O_2} over SnO_2/Sn(l), it should be first heated to a temperature beyond 815 K for sufficient time.

3.2. e.m.f. studies

Attempts were made to measure the e.m.f. of cell (I) at 710 K. The choice of this temperature (710 K) was based on a recent coulometric study on SnO by Yang et al. [23], according to whom Sn_3O_4 coexisted with Sn(l) over a narrow range of temperature between 696 and 731 K. Unfortunately, the impedance of the cell was too high to enable such measurements. Subsequently, the temperature was raised to 753 K which was still about 60 K lower than the disproportionation temperature from DTA (at 20 K/min heating rate). At this temperature, there was a build up of e.m.f. up to 6–7 mV which eventually decayed to a null e.m.f. within 2 h. The temperature was then raised in steps of 25 up to 1000 K. Throughout this range 753–1000 K, only a null e.m.f. ($0 \pm 1.0\,\text{mV}$) could be recorded upholding the coexistence of Sn(l) with SnO_2 in the anode as well, so as to be identical with the phases in the cathode side.

Having established from cell (I) that SnO disproportionates into a coexisting mixture of Sn(l) and SnO_2, the remaining cells (II) and (IV) (wherein SnO constituted the main test electrode material) were first heated to about 1000 K for a few hours to ensure true biphasic equilibrium in the test electrode prior to e.m.f. measurements during subsequent thermal cycles.

The e.m.f. results from cells (II) and (IV) are listed in Table 2. To facilitate the conversion of the reference state of oxygen from N_2/Pt electrode bearing about 10^{-3} atm of oxygen, the e.m.f. of cell (III) was measured over the range 788–965 K (Table 3) and the least-squares expression for these values was derived to be

$$E_{(\text{III})} \pm 2.6\,(\text{mV}) = -2.2 + 0.0921T\,(\text{K}) \tag{1}$$

For further correction of the standard state of oxygen in the reference air/Pt electrode, a P_{O_2} of 0.2088 atm was assumed for dry air. The e.m.f. results on cell (III) were obtained by making use of the same two compartment assembly as in the case of cell (II) in order to minimise systematic errors. Thus, the e.m.f. readings on cell (II) given in Table 2 were corrected for the standard state of oxygen in the reference electrode by combining with e.m.f. values interpolated from Eq. (1) followed by correction for the P_{O_2} of air. Likewise, the e.m.f. readings on cell (IV) (Table 2) were corrected for the standard state of oxygen in the reference Fe/Fe_xO electrode by interpolating numerical values of ΔG^0_f (from literature [24]) at the temperatures at which e.m.f. values were recorded. In this manner, the 60 e.m.f. readings in Table 2 were converted into corresponding values of e.m.f. for the hypothetical cell

$$\text{Pt}, \text{Sn(l)}, \text{SnO}_2 \parallel \text{O}_2\,(P_{O_2} = 1\,\text{atm}), \text{Pt} \tag{V}$$

and are plotted in Fig. 1.

Table 2
Measured e.m.f. results for cells (II) and (IV)

Cell[a]	T (K)	E (mV)
(II)A	801.2[b]	954.45
	954.8	860.13
	874.7	911.43
	1139.8	737.31
	923.0	880.20
	859.3	921.52
	1094.3	769.10
	938.4	869.69
	758.4[b]	985.24
	1048.4	799.53
	891.0	901.19
	825.1	944.11
	1018.6	819.61
	841.6	933.26
(II)B	816.9[b]	944.56
	1079.5	779.22
	1109.9	758.83
	883.8	903.05
	900.4	892.31
	1033.5	809.51
	970.0	849.76
	947.2	862.42
(II)C	808.6	955.13
	791.6	966.16
	985.5	839.62
	833.2[b]	934.54
	932.4	872.02
	867.4[b]	912.86
	1124.3	748.19
	906.4	890.56
	1064.7	788.71
	916.4	882.19
	776.2	975.90
	1002.8	829.59
(IV)A	878.1	50.00
	1135.7	97.75
	1109.0	93.33
	947.7	61.82
	1206.0	111.72
	1122.0	94.91
	971.7	66.44
	900.4	53.49
	1179.2	106.42
	1052.2	80.23
	1013.3	71.16
	1065.5	84.54
	1036.8	77.31
	827.2	36.33
	1166.8	103.74
	1083.0	87.35
(IV)B	853.0	44.58
	772.3	28.87
	1150.6	100.76
	1193.2	109.33
	1021.4	75.88
	997.2	71.12
	923.6	57.76
	1086.1	88.66
	1104.6	91.66
	1058.8	82.44

[a] Cell (II): N_2 ($P_{O_2} \approx 10^{-3}$ atm)/Pt as reference; cell (IV): Fe/Fe$_x$O reference electrode.

[b] Values rejected for the least-squares analysis as a result of wide scatter exhibited by them in third-law treatment.

Prior to the least-squares analysis of the 60 data points, it was necessary to eliminate those which were not consistent with calorimetric data in the literature. For this purpose, a third-law analysis of the e.m.f. results was adopted. The values of the standard enthalpy of formation, $\Delta H^0_{f,298}$ of SnO_2 were derived from such a third-law treatment of the e.m.f. values making use of the free-energy functions (FEFs) for SnO_2(s) and the elements compiled by Lamoreaux et al. [25]. These authors listed the expressions of FEFs for SnO_2(s), Sn(l) and O_2(g) as five term fits valid up to 1000 K and as other such polynomial fits for temperatures extending far beyond 1000 K. To facilitate interpolation, ΔFEF (for the formation reaction of SnO_2(s) from Sn(l) and O_2(g)) was fitted into

Table 3
Experimental results for the cell (III): Pt, N_2 ($P_{O_2} \approx 10^{-3}$ atm) |15 YSZ|air ($P_{O_2} = 0.21$ atm), Pt

Run	T (K)	E (mV)
1	797.2	68.44
	833.2	72.56
	853.8	79.64
	902.9	80.55
2	886.2	83.20
	964.7	86.08
	787.8	70.78
	872.9	75.78
	820.7	75.62
	897.8	78.30

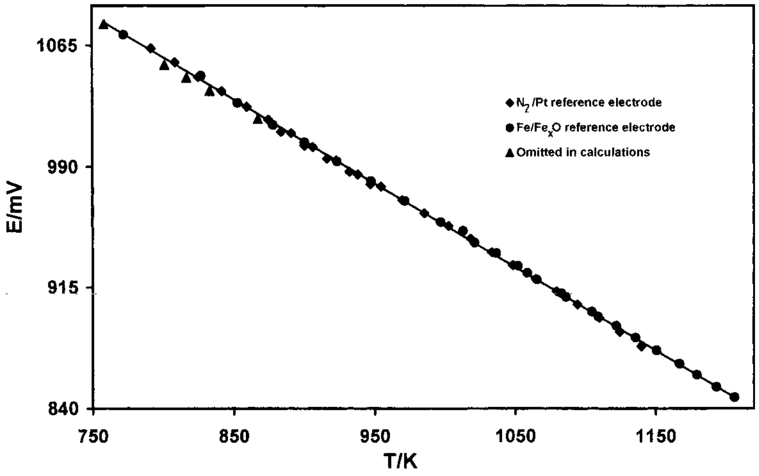

Fig. 1. e.m.f. results of the hypothetical cell (V): Pt, Sn(l), SnO$_2$ || O$_2$ (P_{O_2} = 1 atm), Pt.

two term expressions as follows:

$$\Delta\text{FEF}\,(\text{J K}^{-1}\,\text{mol}^{-1}) = -210.8 + 0.0008T\,(\text{K});\quad (700\text{–}1000\,\text{K}) \qquad (2a)$$

$$\Delta\text{FEF}\,(\text{J K}^{-1}\,\text{mol}^{-1}) = -208.4 - 0.0017T\,(\text{K});\quad (1000\text{–}1200\,\text{K}) \qquad (2b)$$

The values of $\Delta H^0_{f,298}$ were computed using the equation

$$\Delta H^0_{f,298} = \Delta G^0_f - T\Delta\text{FEF} \qquad (3)$$

These values so calculated from Eq. (3) using ΔFEF values (interpolated at the 60 experimental temperatures) are plotted against experimental temperature in Fig. 2. The standard deviation about the mean was calculated to be ±1.3 kJ mol^{-1} after omitting five data points (denoted by “b” in Table 2). Thus, a value of −578.3 kJ mol^{-1} could be assigned for $\Delta H^0_{f,298}$ of SnO$_2$(s). To estimate the overall uncertainty in $\Delta H^0_{f,298}$, an algebraic sum of ±1.3 (from Fig. 2), ±2.2 kJ for $\Delta G^0_f(\text{SnO}_2)$ (from Eq. (6); see later) and that associated with ΔFEF had to be taken into account. Therefore, an uncertainty of ±4.0 kJ could be

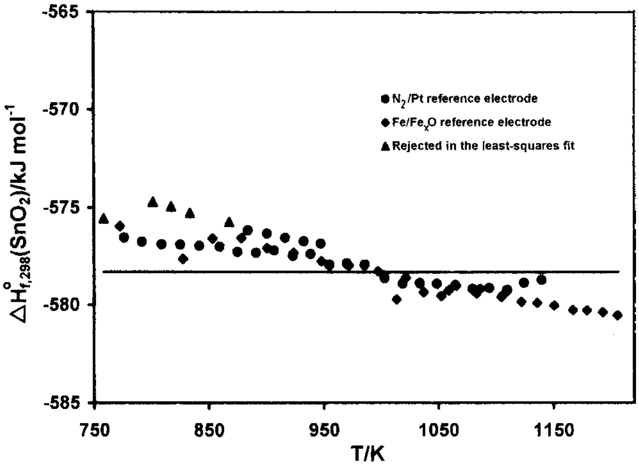

Fig. 2. $\Delta H^0_{f,298}(\text{SnO}_2)$ determined by third-law computations from the e.m.f. data.

ascribed to the value of $-578.3\,\mathrm{kJ\,mol^{-1}}$ for the standard enthalpy of formation of SnO_2(s) at 298 K.

The third-law analysis thus provided a means for eliminating five points out of the 60 listed in Table 2 for the computation of a least-squares expression for the e.m.f. values of the hypothetical cell (V) which is given as follows:

$$E_{(\mathrm{V})} \pm 5.8\,(\mathrm{mV}) = 1474.1 - 0.5201T\,(\mathrm{K}) \qquad (4)$$

valid over the range 772–1206 K.

Corresponding to 4 F of electricity the overall virtual cell reaction for cell (V) could be represented as

$$\mathrm{Sn(l)} + \mathrm{O_2(g)} \rightleftharpoons \mathrm{SnO_2(s)} \qquad (5)$$

The Gibbs energy change for reaction (5) (also equal to ΔG_f^0 of SnO_2(s)) was therefore computed using the familiar Nernst equation ($\Delta G_f^0 = -4FE$):

$$\Delta G_f^0(\mathrm{SnO_2}) \pm 2.2\,(\mathrm{kJ\,mol^{-1}}) = -568.9 + 0.2007T\,(\mathrm{K}) \qquad (6)$$

Bannister [18], who employed Pt or $[\mathrm{Pt} + (\mathrm{U_{0.38}Sc_{0.62}})\mathrm{O}_{2\pm x}]/\mathrm{N_2}$ ($P_{O_2} \approx 10^{-3}$ atm) as the reference electrode for determining the oxygen potential of Sn/SnO_2, had also reviewed nine earlier reports on such e.m.f. measurements. To assess the agreement of Eq. (6) from the present investigation with those reported in the literature by employing similar e.m.f. technique, a plot of ΔG_f^0 is given in Fig. 3. It may be noted that only those studies which were carried out over a temperature range overlapping to a large extent with the present one are compared in this figure. It is seen that the present line for ΔG_f^0 of SnO_2(s) is in close agreement with that found by Bannister [18]. The other four e.m.f. studies yielded values of ΔG_f^0 which are within 2 kJ more negative (at the mean temperature of measurements) than those from Bannister and the present investigation. It should be highlighted that all the 10 different e.m.f. measurements reported in the literature were made with Sn(l)/SnO_2 as the starting material, whereas the present investigation alone had made use of SnO/SnO_2 as the initial electrode material which upon equilibration at or above 753 K resulted in the coexistence of Sn(l)/SnO_2.

The approach of the Sn/SnO_2 equilibrium starting from SnO/SnO_2 in contrast to all other e.m.f. measurements which were directly on Sn/SnO_2 helped to assess the accuracy of the data as much as the precision of the e.m.f. technique. Confirmation of the Sn/Sn_3O_4 equilibrium which was reported to be existing over a narrow range 696–731 K, as reported from the coulometric study by Yang et al. [23] could not be made owing to high impedance of the cell (II) at such lower temperatures. The $\log P_{O_2}$ of Sn/SnO_2 derived from Eq. (6) could be represented as follows:

$$\log P_{O_2} \pm 0.12\,(\mathrm{atm}) = 10.484 - 29719T\,(\mathrm{K}) \qquad (7)$$

This equation could be of help in the choice of a buffer mixture for a lower range of $\log P_{O_2}$ in controlled atmosphere synthesis of advanced materials because

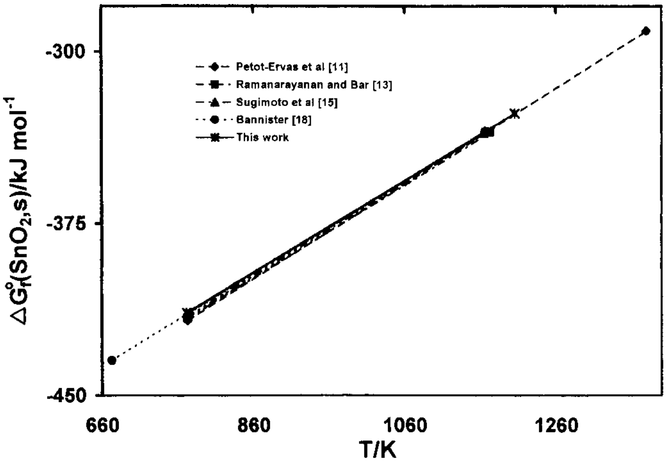

Fig. 3. Standard Gibbs energy of formation of SnO_2(s) from e.m.f. measurements.

of the ease of bubbling a cover gas through liquid tin (melting temperature: 505 K).

This investigation had provided clear evidence through both DTA and e.m.f. studies for the disproportionation of SnO into Sn(l) and SnO_2 at or above 753 K. Further, these studies yielded ΔG_f^0 values for SnO_2(s) in close agreement with those reported by Bannister. In addition, approach of Sn/SnO_2 equilibrium starting with SnO/SnO_2 facilitated an assessment of the accuracy of the e.m.f. measurements. A value of $-578.3 \pm 4.0\,kJ\,mol^{-1}$ could be derived for $\Delta H^0_{f,298}$ of SnO_2(s) from these studies in close agreement with $-577.6 \pm 0.2\,kJ\,mol^{-1}$ reported from a calorimetric study by Lavut et al. [26].

Acknowledgements

The authors are deeply indebted to Dr. V.S. Raghunathan, Associate Director, Materials Characterisation Group, Dr. Baldev Raj, Director, Materials, Chemistry and Reprocessing Group, Dr. P. Rodriguez, Director, IGCAR and to Rev. Dr. John Pragasam, Director, LIFE, Loyola College, for their keen interest and constant encouragement throughout the course of this work. Support from BRNS grant for this research work is gratefully acknowledged.

References

[1] B. Yan, B. Zhu, Xi'an Jiaotong Daxue Xuebao 29 (1995) 20.
[2] A.M. Edwin Suresh Raj, C. Mallika, K.S. Nagaraja, O.M. Sreedharan, Mater. Res. Bull., 36 (2001).
[3] F. Gauzzi, B. Verdini, J. Mater. Sci. Lett. 4 (1985) 1492.
[4] V.M. Glazov, A.S. Pashinkin, A.S. Malkova, V.V. Zharov, Zh. Fiz. Khim. 64 (1990) 811.
[5] V.P. Stets, V.P. Karlov, G.N. Butuzov, A.A. Ryabukha, Poroshk. Metall. 11 (1989) 10.
[6] G.F. Ceccaroni, F. Gauzzi, S. Missori, Thermochim. Acta 165 (1990) 301.
[7] M.S. Moreno, R.C. Mercader, A.G. Bibiloni, J. Phys. Condens. Mater. 4 (1992) 351.
[8] N.I. Dolotov, A.B. Zil'berman, Yu.A. Il'in, A.V. Makhin, V.A. Moshnikov, D.A. Yas'kov, Neorg. Mater. 30 (1994) 83.
[9] T.N. Belford, C.B. Alcock, Trans. Faraday Soc. 61 (1965) 443.
[10] T. Oishi, T. Hiruma, J. Moriyama, Nippon Ginzaku Gakkaishi 36 (1972) 481.
[11] G. Petot-Ervas, R. Farhi, C. Petot, J. Chem. Thermodyn. 7 (1975) 1131.
[12] S. Seetharaman, L.-I. Staffansson, Scand. J. Metall. 6 (1977) 143.
[13] T.A. Ramanarayanan, A.K. Bar, Metall. Trans. B 9 (1977) 485.
[14] M. Iwase, M. Yasuda, S. Miki, T. Mori, Trans. Jpn. Inst. Met. 19 (1978) 654.
[15] E. Sugimoto, S. Kuwata, Z. Kozuka, Nippon Kogyo Kaishi 98 (1982) 429.
[16] I. Karakaya, W.T. Thompson, Can. Metall. Quart. 22 (1983) 61.
[17] R. Kammel, J. Osterwald, T. Oishi, Metallwiss. Tech. 37 (1983) 141.
[18] M.J. Bannister, J. Chem. Thermodyn. 18 (1986) 455.
[19] C. Mallika, R. Pankajavalli, O.M. Sreedharan, Electrochim. Acta 31 (1986) 885.
[20] C. Mallika, O.M. Sreedharan, Thermochim. Acta 190 (1991) 217.
[21] C. Mallika, O.M. Sreedharan, Mater. Lett. 22 (1995) 5.
[22] F. Gauzzi, B. Verdini, A. Maddalena, G. Principi, Inorg. Chim. Acta 104 (1985) 1.
[23] L.-Z. Yang, Z.-T. Sui, C.-Z. Wang, J. Solid State Chem. 113 (1994) 221.
[24] R.A. Giddings, R.S. Gordon, J. Am. Ceram. Soc. 56 (1973) 111.
[25] R.H. Lamoreaux, D.L. Hildenbrand, L. Brewer, J. Phys. Chem. Ref. Data 16 (1987) 419.
[26] E.G. Lavut, B.I. Timofeyev, V.M. Yuldasheva, E.A. Lavut, G.L. Galchenko, J. Chem. Thermodyn. 13 (1981) 635.